

Theoretical Investigations of CO₂ and CH₄ Sorption in an Interpenetrated Diamondoid Metal–Organic Material

Tony Pham,[†] Katherine A. Forrest,[†] Brant Tudor,[†] Sameh K. Elsaidi,^{†,‡} Mona H. Mohamed,^{†,‡} Keith McLaughlin,[†] Christian R. Cioce,[†] Michael J. Zaworotko,^{†,§} and Brian Space*,[†]

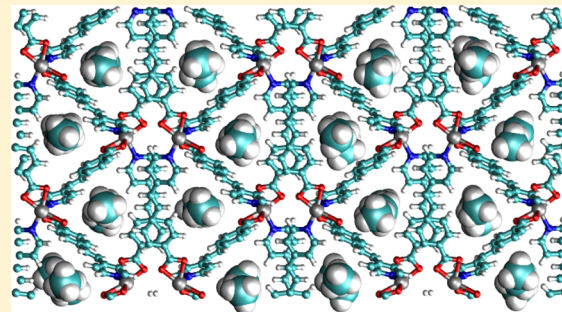
[†]Department of Chemistry, University of South Florida, 4202 East Fowler Avenue CHE205, Tampa, Florida 33620-5250, United States

[‡]Chemistry Department, Faculty of Science, Alexandria University, P.O. Box 426, Ibrahimiya, Alexandria 21321, Egypt

[§]Department of Chemical and Environmental Sciences, University of Limerick, Castletroy, Co., Limerick, Ireland

S Supporting Information

ABSTRACT: Grand canonical Monte Carlo (GCMC) simulations of CO₂ and CH₄ sorption and separation were performed in dia-7i-1-Co, a metal–organic material (MOM) consisting of a 7-fold interpenetrated net of Co²⁺ ions coordinated to 4-(2-(4-pyridyl)ethenyl)-benzoate linkers. This MOM shows high affinity toward CH₄ at low loading due to the presence of narrow, close fitting, one-dimensional hydrophobic channels—this makes the MOM relevant for applications in low-pressure methane storage. The calculated CO₂ and CH₄ sorption isotherms and isosteric heat of adsorption, Q_{st}, values in dia-7i-1-Co are in good agreement with the corresponding experimental results for all state points considered. The experimental initial Q_{st} value for CH₄ in dia-7i-1-Co is currently the highest of reported MOM materials, and this was further validated by the simulations performed herein. The simulations predict relatively constant Q_{st} values for CO₂ and CH₄ sorption across all loadings in dia-7i-1-Co, consistent with the one type of binding site identified for the respective sorbate molecules in this MOM. Examination of the three-dimensional histogram showing the sites of CO₂ and CH₄ sorption in dia-7i-1-Co confirmed this finding. Inspection of the modeled structure revealed that the sorbate molecules form a strong interaction with the organic linkers within the constricted hydrophobic channels. Ideal adsorbed solution theory (IAST) calculations and GCMC binary mixture simulations predict that the selectivity of CO₂ over CH₄ in dia-7i-1-Co is quite low, which is a direct consequence of the MOM's high affinity toward both CO₂ and CH₄ as well as the nonspecific mechanism shown here. This study provides theoretical insights into the effects of pore size on CO₂ and CH₄ sorption in porous MOMs and its effect upon selectivity, including postulating design strategies to distinguish between sorbates of similar size and hydrophobicity.



I. INTRODUCTION

Methane (CH₄) is considered a desirable alternative for energy-related applications because it burns cleaner than gasoline and diesel fuels, and it is widely available in many countries in the form of natural gas.¹ Currently, methane-containing natural gas is mainly stored as compressed natural gas (CNG) at pressures greater than 200 atm within tanks that require an expensive multistage compression.² Although CNG vehicles already exist in some countries, it is notable that these current CNG tanks are heavy, expensive, and potentially combustible.¹ A possible alternative to CNG is adsorbed natural gas (ANG) where the gas is stored as an adsorbed phase in a porous solid at lower pressures.^{2,3} However, porous materials that are commercially available today (e.g., activated carbons) do not have sufficiently high storage capacities for CH₄ at low pressures.³

In response to these environmental issues and technological challenges, the scientific and engineering communities have reported a number of novel porous materials, called metal–

organic materials (MOMs), which have been demonstrated to be strong candidates for applications in gas storage and separation.^{3–6} MOMs are solid crystalline compounds that are synthesized from metal ions (or metal-ion clusters) and molecular bridging ligands. The building block approach allows for the possibility to create a large number of MOM structures.^{7,8} As a result, a variety of MOMs with different pore sizes, dimensions, chemical functionalities, and topologies have been synthesized.^{8,9} Most MOMs of interest contain three-dimensional structures that include uniform pores and channels that can be used to sorb guest molecules, such as H₂, CO₂, and CH₄.^{1,4,10} A subset of MOMs have been shown to display remarkable potential for industrial applications in CO₂ capture/storage and separations.^{11–14} In addition, a number of

Received: March 14, 2014

Revised: May 13, 2014

Published: May 16, 2014

MOMs have the capability to store large amounts of CH_4 at near-ambient temperatures and high pressures. Indeed, some MOMs have already been demonstrated to surpass the old U.S. Department of Energy (DOE) target for on-board methane storage,^{3,15–21} which is 180 v(STP)/v under 35 bar and near-ambient temperature.²² Note, this target was recently modified to 263 v(STP)/v under the same conditions,²³ and currently, no MOM surpasses this value for methane storage.²⁴

Recent studies have shown that there are several factors that influence gas uptakes in MOMs. For instance, MOMs that contain open-metal sites or amine functional groups were shown to exhibit high uptakes and initial isosteric heats of adsorption, Q_{st} , for various gas molecules.^{11,20,25–27} However, some of the disadvantages of MOMs that have these chemical functionalities are that they can interact with water, which hinder these materials for industrial applications in gas separations, and there can be high energy costs associated with activating and regenerating the material.^{13,28} Porous MOMs that contain saturated metal centers (SMCs) are a promising alternative to the aforementioned MOMs. These materials rely on strong physisorption interactions between the sorbate molecules and the framework rather than, e.g., metal–sorbate coordination. In addition, these MOMs are beneficial in the context of activation and regeneration as well as displaying remarkable water stability. Pillared square grids that contain primitive cubic (pcu) topology^{12,13,29} and MOMs with mmo topology^{14,30} are examples of porous MOMs that contain SMCs.

Diamondoid (dia) networks are one of the earliest examples of MOMs that are designed via a crystal engineering approach^{31,32} that do not contain open-metal sites or amine functional groups but have controllable pore sizes. They are based upon 4-connected tetrahedral nodes and linear linkers that form a three-dimensional net.^{33,34} Diamondoid networks are amenable to fine-tuning with regards to both pore size and chemical functionality. The pore size of these MOMs can be tuned through linker length and/or interpenetration, while the functionality can be adjusted by introducing functional groups on the linker. It is noteworthy that MOMs within this platform have the tendency to interpenetrate, which results in a 3D framework with one-dimensional pores.^{35–38} The degree of interpenetration can often be controlled through the choice of solvent used to synthesize the MOM. The more highly interpenetrated structure results in a framework with smaller pore sizes.

dia-7i-1-Co is a recently synthesized MOM that exhibits the aforementioned diamondoid topology.³⁹ It consists of a 7-fold interpenetrated net of Co^{2+} ions coordinated to 4-(2-(4-pyridyl)ethenyl)benzoate ligands (Figure 1). The highly interpenetrated network of this MOM as well as the nonpolar nature of the linker contributes to narrow one-dimensional hydrophobic pores. Indeed, the pore limiting diameter (PLD) of this MOM was measured to be 5.28 Å. The PLD embodies the accessible pore size of the material and it is obtained by measuring the longest diagonal of the channel and subtracting 3.5 Å corresponding to van der Waals distances. Although there are other synthesized diamondoid MOMs that contain smaller PLDs (e.g., dia-8i-1 and dia-5i-3), dia-7i-1-Co is the smallest member that is porous and can be used to sorb guest species. Thus, dia-7i-1-Co is a MOM that is of interest to experimentalists for its gas sorption and separation properties. This MOM is also of interest to theoretical chemists to study the effects of pore size on gas sorption through subsequent

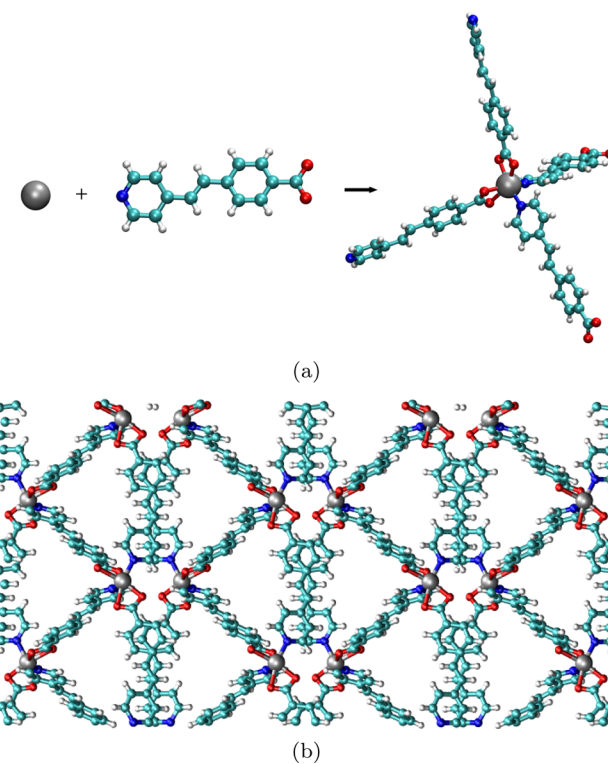


Figure 1. (a) Scheme showing the assembly of the tetrahedral node in dia-7i-1-Co. (b) Shifted c -axis view of the $2 \times 2 \times 2$ unit cell system of dia-7i-1-Co. Atom colors: C = cyan, H = white, N = blue, O = red, Co = silver.

modeling studies and to assess the selectivity achievable through such a platform.

Experimental studies have shown that the initial (zero-coverage) Q_{st} for CO_2 for dia-7i-1-Co is approximately 30 kJ mol⁻¹.³⁹ This CO_2 Q_{st} value is greater than most MOMs that contain open-metal sites, such as HKUST-1⁴⁰ and various *rht*-metal–organic frameworks,⁴¹ as well as pillared square grids that contain inorganic fluoroanions.^{12,29} It is notable that the aforementioned MOMs rely on metal–sorbate interactions and physisorption with inorganic fluoroanions, respectively, for CO_2 sorption. In dia-7i-1-Co, only narrow hydrophobic channels exist within the MOM, so the high Q_{st} for CO_2 in this compound must be attributed to a strong physisorptive interaction with the constricted pores.

Experimental studies have also demonstrated that dia-7i-1-Co has a high uptake capacity for CH_4 at low loading.³⁹ Moreover, the initial Q_{st} value for CH_4 was shown to be very high through experimental measurements. Indeed, depending on the empirical fitting method used, the initial CH_4 Q_{st} value was found to be in the range 22.5–28.0 kJ mol⁻¹ for dia-7i-1-Co. Applying the virial method⁴² on the experimental CH_4 sorption isotherms yielded an initial Q_{st} value of 24.0 kJ mol⁻¹.³⁹ This value is considerably higher than those found for CH_4 sorption in covalent–organic frameworks (COFs) and MOMs with open-metal sites. In addition, a literature survey of MOMs with high Q_{st} values for CH_4 reveals that the aforementioned value for dia-7i-1-Co is currently the highest of all MOMs synthesized thus far.^{6,24,39} Note, although the MOM PCN-14 was originally shown to exhibit a CH_4 Q_{st} value of approximately 30 kJ mol⁻¹ at initial loading,¹⁵ recent studies have demonstrated that this MOM exhibited an initial value of 18.7 kJ mol⁻¹.²⁴

In this work, we use grand canonical Monte Carlo (GCMC) methods to investigate CO_2 and CH_4 sorption and separation in dia-7i-1-Co. Simulated sorption isotherms and Q_{st} values for both sorbate molecules are presented and compared to the corresponding experimental results. It will be shown that good agreement with experiment for CO_2 and CH_4 sorption is obtained for dia-7i-1-Co. Further, insights into the reason for high uptake capacity for CH_4 in this compound at low loading will be obtained. It will be demonstrated from a theoretical point of view that MOMs with narrow pore sizes are beneficial for gas sorption at low loading. Although without further considerations, e.g., chemical modifications/decorations, MOMs may only exhibit selectivity based on size and hydrophobicity.

The hydrophobic character of dia-7i-1-Co contributes to the MOM's stability in moisture as well as its remarkable stability under practical conditions. The fact that this MOM is stable in humid environments makes it advantageous over MOMs with open-metal sites or amine functional groups for industrial applications in gas separations where the presence of water vapor must be dealt with. However, because dia-7i-1-Co has high affinity toward both CO_2 and CH_4 , the capability of this MOM to separate CO_2 from CH_4 in gas mixtures, such as biogas or natural gas, will be rather limited. Indeed, it will be shown through ideal adsorbed solution theory (IAST)⁴³ and GCMC calculations that dia-7i-1-Co has a low selectivity for CO_2 over CH_4 .

II. METHODS

Simulations of CO_2 and CH_4 sorption in dia-7i-1-Co were performed using GCMC methods. This method entails constraining the chemical potential, volume, and temperature to be constant while allowing the particle number and other statistical mechanical quantities to fluctuate.⁴⁴ The simulation involves the random insertion, deletion, and movement of sorbate molecules with acceptance or rejection based on a random number generator scaled by the energetic favorability of the move. The average particle number was calculated numerically by a statistical mechanical expression based on the grand canonical ensemble.⁴⁵ The chemical potential for both CO_2 and CH_4 was determined for a range of temperatures through the Peng–Robinson equation of state.⁴⁶ All simulations were performed in a rigid $2 \times 2 \times 2$ unit cell system of the MOM as shown in Figure 1b. A spherical cutoff distance corresponding to half the shortest system cell dimension length was used for the simulations.

The total potential energy of the MOM–sorbate system was calculated as the sum of the repulsion/dispersion and electrostatic energies through the use of the Lennard-Jones 12–6 potential and Ewald summation,⁴⁷ respectively. Note, in previous work, our group focused on the importance of explicit many-body polarization interactions for simulations in MOMs.^{10,48,49} However, dia-7i-1-Co is a MOM that contains constricted hydrophobic channels, which causes van der Waals interactions to dominate as the sorbate molecules interact with the framework in a confined space. Thus, induced dipole effects were negligible for gas sorption in this compound. Similar findings were observed for simulations in other MOMs that have narrow pore sizes.^{9,50} Control simulations in dia-7i-1-Co revealed that, when included, polarization contributes to less than 7% and 4% of the total energy for CO_2 and CH_4 sorption, respectively, and does not significantly alter the sorption isotherms and associated Q_{st} values. Thus, only van der Waals and electrostatic interactions were considered for the simulations in this work. Further, long-range corrections were applied to all terms of the potential due to the finite size of the simulation box. The long-range contribution to the Lennard-Jones potential was implemented using a previously reported procedure,⁵¹ while long-range electrostatic interactions was handled by performing full Ewald summation.

The MOM force field for dia-7i-1-Co consists of Lennard-Jones parameters and atomic point partial charges on all atoms of the framework. The Lennard-Jones parameters for all C, H, and N atoms were taken from the optimized potentials for liquid simulations—all atom (OPLS-AA) force field.⁵² This force field contains parameters that are specific for atoms in aromatic systems, which this MOM contains. For Co and O, the Lennard-Jones parameters were taken from the universal force field (UFF).⁵³ The partial charges for the atoms in dia-7i-1-Co were obtained from quantum mechanical calculations on several fragments that were taken from the crystal structure of the MOM. A comprehensive detail of this procedure can be found in the Supporting Information. Nonpolar potentials of CO_2 and CH_4 were used for the simulations in this work; they are denoted $\text{CO}_2\text{-PHAST}$ ⁵⁴ and Me-PHAST ,⁵⁵ respectively. These potentials were developed in our group using a standard sorbate fitting procedure. More details of the sorbate models used in this work can be found in the Supporting Information.

Note, preliminary simulation results were also performed using the TraPPE potentials^{56,57} for the respective sorbates in dia-7i-1-Co. While the TraPPE CH_4 model gave similar isotherms and Q_{st} values to the Me-PHAST model, the isotherms for the TraPPE CO_2 model are qualitatively different than experiment and the $\text{CO}_2\text{-PHAST}$ model. Only the results for the $\text{CO}_2\text{-PHAST}$ and Me-PHAST models are shown in this paper; the reference to the TraPPE potentials was made to report the aforementioned observation.

In GCMC, the Q_{st} values are calculated based on the fluctuations of the particle number, N , and total potential energy, U , in the MOM–sorbate system through the expression⁵⁸

$$Q_{st} = -\frac{\langle NU \rangle - \langle N \rangle \langle U \rangle}{\langle N^2 \rangle - \langle N \rangle^2} + kT \quad (1)$$

where k is the Boltzmann constant and T is the temperature. This is in contrast to the Q_{st} values that are derived experimentally, as these values are typically determined through a finite difference approximation to the Clausius–Clapeyron equation.⁵⁹

For GCMC simulation of binary mixtures of CO_2 and CH_4 in dia-7i-1-Co, the simulations were performed in the ideal gas limit where the fugacities were equal to the partial pressures. Further, the selectivity of one sorbate molecule relative to another was calculated by the expression

$$S = \frac{x_i y_j}{y_i x_j} \quad (2)$$

where x_i and x_j are the mole fractions of components i and j , respectively, in the adsorbed phase and y_i and y_j are the mole fractions of components i and j , respectively, in the bulk phase.

For all state points considered, the simulations consisted of 5×10^6 Monte Carlo steps to guarantee equilibration, followed by an additional 5×10^6 steps to sample the desired thermodynamic properties. All simulations of CO_2 and CH_4 in dia-7i-1-Co were performed using the Massively Parallel Monte Carlo (MPMC) code,⁶⁰ which is currently available for download on Google Code.

III. RESULTS AND DISCUSSION

Figure 2 shows the CO_2 and CH_4 sorption isotherms for experiment and simulation in dia-7i-1-Co at 298 and 273 K. It can be observed that good agreement with experiment was achieved for simulations of CO_2 and CH_4 sorption at both temperatures for the entire low-pressure range considered. The maximum calculated error is $\pm 0.05 \text{ mmol g}^{-1}$ for the modeling studies. Note, it can be seen that, for both sorbate molecules, the simulation slightly oversorbs the experimental results in the very low-pressure region (below 0.20 atm) at both temperatures. This could be due to the fact that it takes some time for the CO_2 and CH_4 molecules to diffuse into the one-dimensional channels in this MOM in experiment at low loading. In GCMC, only the random insertion, deletion, and

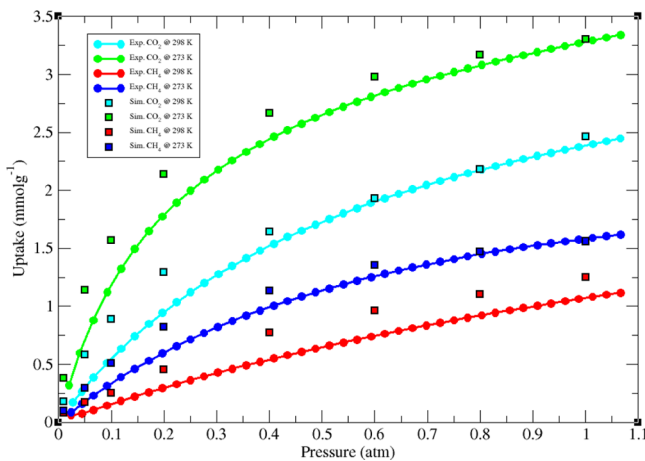


Figure 2. Low-pressure CO₂ and CH₄ sorption isotherms in dia-7i-1-Co for experiment (circle)³⁹ and simulation (square) at 298 K (CO₂ = cyan; CH₄ = red) and 273 K (CO₂ = green; CH₄ = blue).

movement of sorbate molecules are performed, so the effects of transport and associated kinetic phenomena are not an issue. The difference between experiment and simulation at low pressures could also be attributed to the choice of van der Waals parameters that were used for the MOM. As explained in the Methods section, the Lennard-Jones parameters for all MOM atoms were taken directly from known general purpose force fields. The small pore sizes afforded by dia-7i-1-Co cause van der Waals interactions to dominate for gas sorption in this MOM. Thus, the type of repulsion/dispersion parameters used for the MOM will affect the overall potential energy of the MOM–sorbate system. It might be possible to obtain better agreement with experiment at low pressures by using Lennard-Jones parameters that are acquired through electronic structure methods. Such efforts are ongoing in our group.

It is important to emphasize that the CH₄ uptakes in dia-7i-1-Co are rather high at low pressures. At 1.0 atm, the experimental CH₄ uptakes in dia-7i-1-Co are approximately 1.07 mmol g⁻¹ (23.97 cm³ g⁻¹, 33.08 cm³ cm⁻³) and 1.58 mmol g⁻¹ (35.39 cm³ g⁻¹, 48.84 cm³ cm⁻³) at 298 and 273 K, respectively. Note, cm³ cm⁻³ refers to cm³ of sorbate uptake per cm³ of MOM. These uptakes are comparable to the corresponding values that were calculated through simulation. Further, these values are among the highest of reported MOM materials for CH₄ sorption under these conditions.⁶ Though dia-7i-1-Co has high uptake for CH₄ at low pressures, the low surface area of the MOM limits CH₄ sorption at higher pressures. As such, dia-7i-1-Co does not surpass the U.S. Department of Energy (DOE) target for on-board methane storage (263 v(STP)/v under 35 bar and near-ambient temperature).^{23,24} However, dia-7i-1-Co could still be useful for CH₄ storage applications at low pressures (under 5.0 atm).

Figure 3a shows the GCMC-calculated Q_{st} values for the CO₂-PHAST potential compared to the experimental Q_{st} values for CO₂ in dia-7i-1-Co. The former was determined using eq 1, while the latter was determined by applying the virial method⁴² to the experimental CO₂ sorption isotherms at 298 and 273 K. It can be seen that the experimental Q_{st} values for CO₂ in dia-7i-1-Co are relatively constant at about 30 kJ mol⁻¹ as the loading increases. The theoretical Q_{st} values show a similar trend, with values of approximately 31 kJ mol⁻¹ across all loadings. Thus, there is very good agreement between the experimental and simulated Q_{st} values for CO₂. The fact that

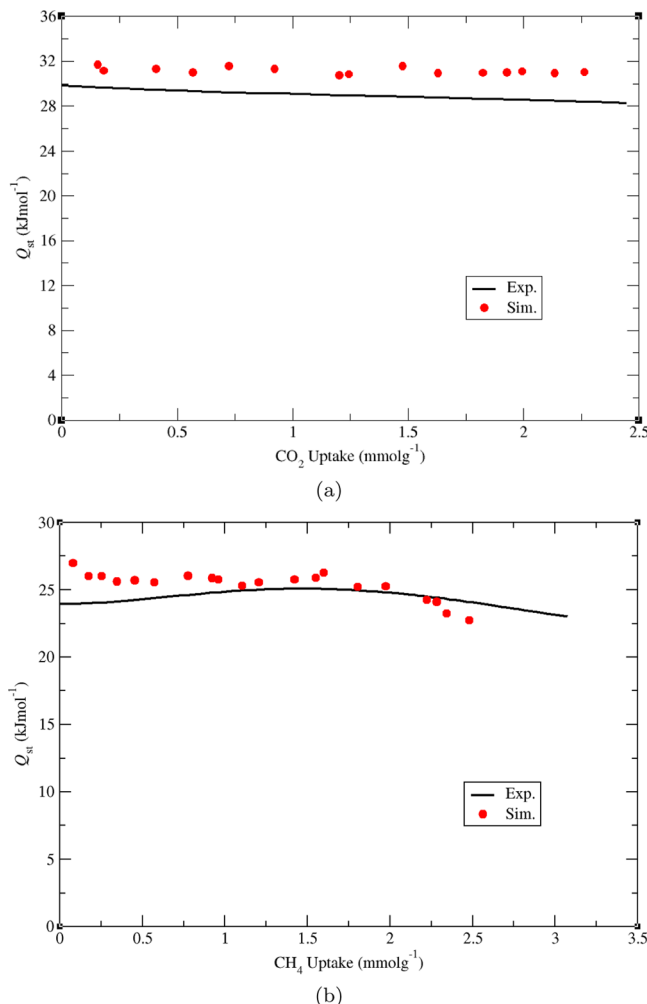


Figure 3. Isosteric heats of adsorption, Q_{st}, for (a) CO₂ and (b) CH₄ plotted against uptakes in dia-7i-1-Co for experiment (black line) and simulation (red circles). The experimental Q_{st} values (taken from ref 39) shown here for both sorbates were calculated using the virial method.

the Q_{st} values for CO₂ are nearly constant for all loadings indicates that there is only one type of binding site for CO₂ in this MOM. The constant Q_{st} values also indicate that sorbate–sorbate interactions do not play a significant role in the energetics for sorption in this MOM. This is in contrast to some other existing MOMs that exhibit increasing Q_{st} behavior with increasing loading for a particular sorbate, thus indicating favorable sorbate–sorbate interactions within the material.^{3,9}

The experimental and GCMC-calculated Q_{st} values for CH₄ in dia-7i-1-Co are shown in Figure 3b. The experimental CH₄ Q_{st} values shown herein were calculated using the virial method.⁴² These values are nearly constant at approximately 24 kJ mol⁻¹ for all loadings. Further, these values are in good agreement with those calculated from GCMC simulation, as the simulated Q_{st} values for CH₄ are roughly constant at approximately 26 kJ mol⁻¹ for virtually all loadings considered. Thus, both the virial method Q_{st} values and simulated results predict the presence of only one type of binding site for CH₄ in this compound. Note, the experimental Q_{st} values for CH₄ in dia-7i-1-Co have also been calculated using different methods, including the Langmuir–Freundlich equation and the Clausius–Clapeyron equation⁵⁹ (see ref 39). In addition, in this

work, the experimental $\text{CH}_4 Q_{st}$ values were also calculated by fitting the experimental CH_4 sorption isotherms at 298 and 273 K to the dual-site Langmuir–Freundlich equation (see Supporting Information).³⁹

Implementing the other fitting methods on the experimental CH_4 sorption isotherms resulted in higher initial Q_{st} values, with values of 27.3, 26.7, and 28.6 kJ mol^{-1} for the Langmuir–Freundlich, Clausius–Clapeyron, and dual-site Langmuir–Freundlich equations, respectively (see Supporting Information).³⁹ However, it can be seen that the Q_{st} values that were calculated using these methods decrease sharply with increasing loading. Nevertheless, both the experimental (considering all fitting methods) and simulated Q_{st} values are within the vicinity of each other across all loadings. In addition, both experiment and simulation predict that the initial Q_{st} value for CH_4 is quite high in this compound. Indeed, the initial Q_{st} value for CH_4 in dia-7i-1-Co is currently the highest out of all MOMs synthesized thus far.

Examination of the full three-dimensional histogram showing the sites of CO_2 and CH_4 sorption in dia-7i-1-Co reveals that there is indeed only one type of binding site for the respective sorbate molecules. The sorbed gas molecules are essentially localized within the center of the one-dimensional hydrophobic channels in this MOM (Figure 4). Inspection of the modeled

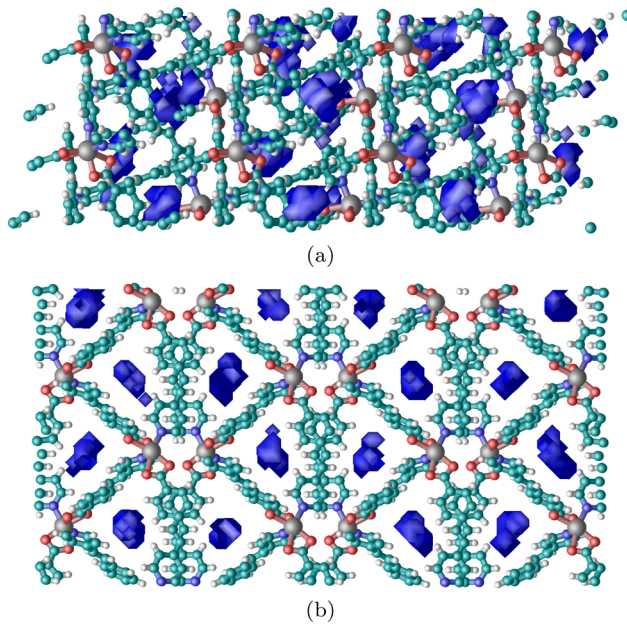


Figure 4. Three-dimensional histogram showing the sites of CO_2 sorption (blue) in dia-7i-1-Co: (a) a -axis view; (b) shifted c -axis view. The sorption sites for CH_4 are similar. Atom colors: C = cyan, H = white, N = blue, O = red, Co = silver.

structure for CO_2 and CH_4 sorption in dia-7i-1-Co reveals that the sorbate molecules can make a favorable interaction with the organic linkers within the confined space of the pores (Figures 5 and 6). This sorption site is clearly dominated by van der Waals interactions, as the sorbate molecules can interact with multiple portions of the framework simultaneously in this region. Evaluation of the energetic contributions for CO_2 and CH_4 sorption from simulation confirmed these findings, as it was found that van der Waals energetics contribute to over 85% and 99% of the total energy for CO_2 and CH_4 sorption, respectively.

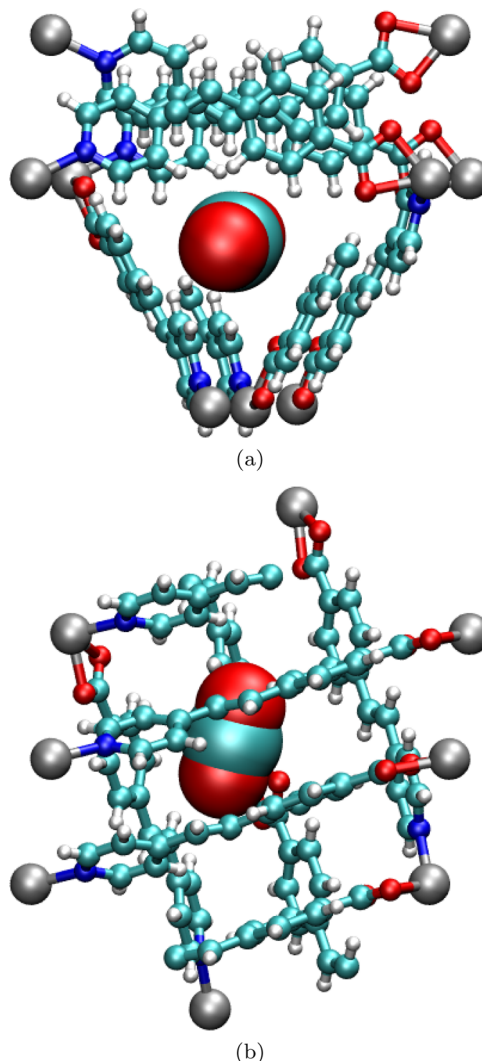


Figure 5. Molecular illustration of the CO_2 sorption site in dia-7i-1-Co: (a) top view; (b) side view. Atom colors: C = cyan, H = white, N = blue, O = red, and Co = silver.

Further, the combination of the narrow space and the hydrophobic nature of the pores explains why the CH_4 uptakes and Q_{st} values are so high in this compound at low loading. Although there are other porous MOMs that contain even smaller pore sizes, such as members of the “SIFSIX” series¹³ and the mmo net series,^{14,30} it is notable that these materials are much less attractive toward CH_4 . This is because these compounds contain polar moieties through the use of SiF_6^{2-} and MO_4^{2-} ($M = \text{Cr}, \text{Mo}, \text{W}$) groups, respectively, which have lower affinity for CH_4 . Thus, a key discovery observed in this study is that the decoration of the pore walls with nonpolar C–H groups increases molecular recognition toward CH_4 . The confined region within the channels is the sorption site for all CO_2 and CH_4 molecules in dia-7i-1-Co, which explains why the GCMC-calculated Q_{st} values are relatively constant across all loadings for the respective sorbate molecules. Note, although the sorbate molecules interact with this MOM primarily through van der Waals interactions, the small contributions from charge–quadrupole interactions were important for enhancing MOM–sorbate interactions in the case of CO_2 sorption. It would be expected that the introduction of polar functional groups on the organic ligand would increase

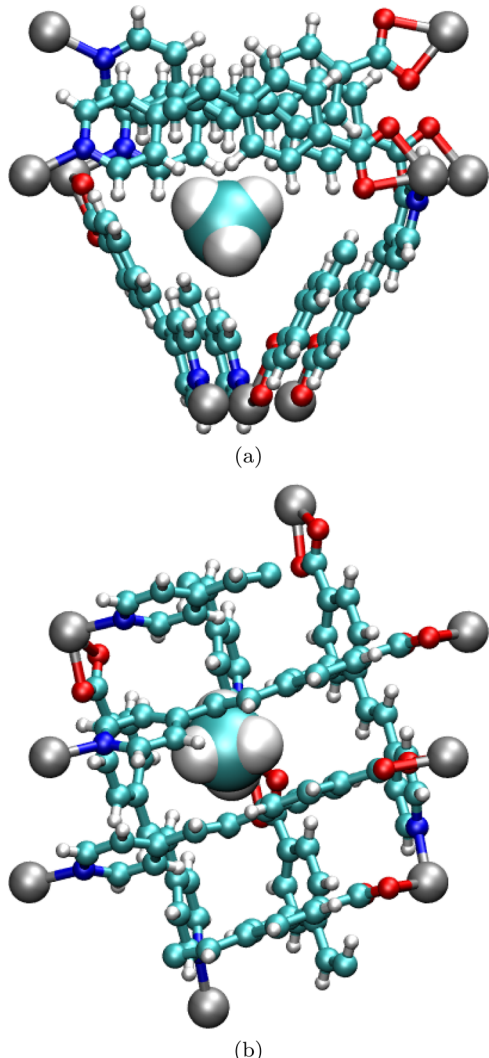


Figure 6. Molecular illustration of the CH_4 sorption site in dia-7i-1-Co: (a) top view; (b) side view. Atom colors: C = cyan, H = white, N = blue, O = red, and Co = silver.

electrostatic interactions even further during sorption. This alteration would result in enhanced binding strength for CO_2 molecules, but also decrease affinity for CH_4 , thus increasing separation capabilities.

Figure 7 shows the GCMC-calculated selectivities of CO_2 over CH_4 within a binary mixture of 50:50 CO_2/CH_4 and 5:95 CO_2/CH_4 in dia-7i-1-Co at 298 K and pressures up to 1.0 atm. These mixtures mimic the composition of biogas and natural gas, respectively. The calculated values are compared to the corresponding selectivities that were determined by implementing IAST⁴³ on the experimental and simulated CO_2 and CH_4 single-component sorption isotherms. More details of the IAST calculations can be found in the Supporting Information. The binary mixture simulations predict that the selectivity of CO_2 over CH_4 slightly decreases with increasing loading for both mixture compositions in dia-7i-1-Co. A CO_2/CH_4 selectivity of 3.5 and 3.1 was calculated at 1.0 atm through the GCMC simulations for the 50:50 CO_2/CH_4 and 5:95 CO_2/CH_4 mixtures, respectively. In contrast to the binary mixture simulations, IAST calculations on the experimental and simulated isotherms show slightly increasing selectivity with increasing loading in dia-7i-1-Co for the pressure range shown.

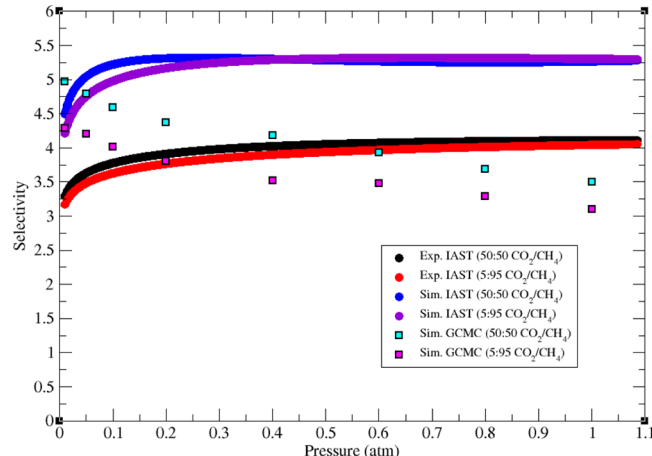


Figure 7. Calculated selectivities of CO_2 over CH_4 as determined through ideal adsorbed solution theory (IAST) calculations on the experimental and simulated single-component sorption isotherms in a 50:50 CO_2/CH_4 (experimental = black circles, simulated = blue circles) and 5:95 CO_2/CH_4 mixture (experimental = red circles, simulated = violet circles) in dia-7i-1-Co at 298 K and pressures up to 1.0 atm. The selectivities calculated from grand canonical Monte Carlo (GCMC) binary mixture simulations (50:50 CO_2/CH_4 = cyan squares, 5:95 CO_2/CH_4 = magenta squares) are also shown.

This difference in the shape of the selectivity plot can be attributed to the fitting parameters that were used to calculate the selectivities using IAST or that IAST is inadequate here due to the disparate sorbate interactions and/or the sorption mechanisms in the confined space. IAST is a very useful qualitative guide for MOF sorption studies, but it is difficult to predict *a priori* when it will be quantitatively effective and what exactly breaks down when it fails. Indeed, it was conceived as a framework to calculate activity coefficients that were subsequently found to be order unity.⁴³

It can be observed that the experimental IAST selectivities increase slightly with increasing loading until about 0.30 atm. Afterward, the CO_2/CH_4 selectivity remains relatively constant as the pressure continues to increase for both mixture compositions. IAST calculations on the experimental isotherms predict a CO_2/CH_4 selectivity of 4.1 and 4.0 at 1.0 atm for the 50:50 CO_2/CH_4 and 5:95 CO_2/CH_4 mixtures, respectively, in dia-7i-1-Co. The simulated IAST selectivities for both mixtures are higher than the corresponding experimental IAST selectivities at all pressures, and the increase in the selectivities within the low-pressure region is still noticeable. The selectivities for the former are higher than those for the latter at all pressures possibly because GCMC simulations of single-component CO_2 and CH_4 sorption in dia-7i-1-Co predict notably higher uptake than experiment for the respective sorbate molecules in this loading range at all pressures considered up to 1.0 atm. The simulated IAST selectivities are relatively constant starting at approximately 0.30 atm, and a value of 5.3 at 1.0 atm was obtained for both the 50:50 CO_2/CH_4 and 5:95 CO_2/CH_4 mixtures. Note, the IAST selectivities for both experiment and simulation at low loading were found to be in good agreement with the selectivities that were obtained based on the ratio of the Henry's law constant for the respective sorbates in the low-pressure region. Using Henry's law, the CO_2/CH_4 selectivities based on the experimental and simulated isotherms are 3.7 and 4.2, respectively. For all methods of calculating the CO_2/CH_4 selectivities, it can be

seen that the selectivities are slightly higher for the 50:50 mixture compared to the 5:95 mixture, especially at low loadings. These results suggest that the material can separate CO₂ more efficiently if a greater concentration of CO₂ is present.

It can be observed that the simulated IAST selectivities and the binary mixture selectivities are in good agreement with each other at very low loadings for both mixture compositions. However, the selectivities that were calculated by applying IAST on the simulated sorption isotherms are notably higher than those that were calculated through the binary mixture simulations across most of the considered pressure range. Thus, even though both methods involve simulations of CO₂ and CH₄ in the MOM, the fact that the IAST-calculated selectivities are different from the binary mixture selectivities suggests that the former may be a consequence of the dependence of the fitting parameters/models that are used. It also is true that IAST, while often a reasonable guide, can fail quantitatively, especially in some of the most interesting systems that involve strong, heterogeneous interactions. Nevertheless, the IAST- and GCMC-calculated selectivities are within the vicinity of each other for all pressures considered to within joint uncertainties. Overall, the results from the binary mixture simulations and the IAST calculations predict that the selectivity of CO₂ to CH₄ in dia-7i-1-Co at 298 K and 1.0 atm ranges from 3.0 to 5.5, which is quite low compared to most other MOM materials under this condition. Indeed, this can be attributed to the fact that dia-7i-1-Co has high affinity toward both CO₂ and CH₄.

IV. CONCLUSION

In conclusion, a computational study of CO₂ and CH₄ sorption in the 7-fold interpenetrated diamondoid MOM, dia-7i-1-Co, was presented. The simulated sorption isotherms and Q_{st} values reported herein for this MOM were in very good agreement with the experimental measurements for the respective sorbate molecules. The presence of narrow channels in dia-7i-1-Co results in a strong interaction between the CO₂ molecules and the framework. Indeed, the Q_{st} for CO₂ is approximately 30 kJ mol⁻¹ for dia-7i-1-Co, which is comparable to most MOMs that contain open-metal sites or inorganic anions. Further, the hydrophobic nature of these narrow channels corresponds to a high affinity for CH₄. GCMC simulation predicts that dia-7i-1-Co has an initial CH₄ Q_{st} value of approximately 26 kJ mol⁻¹, which is comparable to the values that were derived experimentally. The initial Q_{st} value for CH₄ is currently the highest out of all MOM materials reported thus far. Moreover, the CH₄ uptake in dia-7i-1-Co at 298 K and 1.0 atm is one of the highest among reported MOM materials. Thus, dia-7i-1-Co seems to be a good prototype compound for low-pressure CH₄ storage applications. The three-dimensional histograms showing the sites of occupancy in dia-7i-1-Co reveal that there is only one type of binding site for CO₂ and CH₄, which is essentially localization within the hydrophobic channels.

Overall, this study provided theoretical insights into how MOMs with extremely narrow pore sizes have enhanced binding strength for certain gas molecules. In the case of dia-7i-1-Co, the presence of constricted hydrophobic channels within the MOM is responsible for the increased uptakes at low loading and initial Q_{st} values for CO₂ and CH₄ and for a relatively constant high sorption affinity at all pressures considered. Although dia-7i-1-Co has high sorption capacity for CO₂ and CH₄, the fact that the MOM has high affinity

toward both of these gas molecules implies that this compound has limitations for industrial applications in CO₂ separations, such as biogas treatment and natural gas cleanup. For example, IAST and GCMC calculations predict that the selectivity of CO₂ over CH₄ will be very low for dia-7i-1-Co. Fortunately, this study has also provided insights into creating variant structures for improving the selectivity of one gas relative to another. For instance, it would be expected that the replacement of the ethylene group (C=C) in the organic linker of dia-7i-1-Co with an azo group (N=N) would increase the binding strength and selectivity toward CO₂ and also decrease the affinity toward CH₄, as this alteration would introduce polar functionality within the channels. This phenomenon will be investigated in future experimental and theoretical studies.

■ ASSOCIATED CONTENT

S Supporting Information

Details of the electronic structure calculations, pictures of MOM fragments, tables of properties, details of sorbate models, details of IAST calculations, and additional content. This material is available free of charge via the Internet at <http://pubs.acs.org>.

■ AUTHOR INFORMATION

Corresponding Author

*E-mail: brian.b.space@gmail.com (B.S.).

Author Contributions

T.P. and K.A.F. contributed equally.

Notes

The authors declare no competing financial interest.

■ ACKNOWLEDGMENTS

This work was supported by the National Science Foundation (Award No. CHE-1152362). Computations were performed under a XSEDE Grant (No. TG-DMR090028) to B.S. This publication is also based on work supported by Award No. FIC/2010/06, made by King Abdullah University of Science and Technology (KAUST). The authors also thank the Space Foundation (Basic and Applied Research) for partial support. The authors acknowledge the use of the services provided by Research Computing at the University of South Florida. M.H.M. acknowledges support from the Schlumberger Foundation and its Faculty for the Future Fellowship program. Lastly, the authors thank Professor David S. Sholl for his assistance on the ideal adsorbed solution theory (IAST) calculations.

■ REFERENCES

- (1) Collins, D. J.; Ma, S.; Zhou, H.-C. In *Metal-Organic Frameworks: Design and Application*; MacGillivray, L. R., Ed.; John Wiley & Sons, Inc.: Hoboken, NJ, 2010; pp 249–266.
- (2) Düren, T.; Sarkisov, L.; Yaghi, O. M.; Snurr, R. Q. Design of New Materials for Methane Storage. *Langmuir* **2004**, *20*, 2683–2689.
- (3) Wilmer, C. E.; Farha, O. K.; Yildirim, T.; Eryazici, I.; Krungleviciute, V.; Sarjeant, A. A.; Snurr, R. Q.; Hupp, J. T. Gram-Scale, High-Yield Synthesis of a Robust Metal-Organic Framework for Storing Methane and Other Gases. *Energy Environ. Sci.* **2013**, *6*, 1158–1163.
- (4) Suh, M. P.; Park, H. J.; Prasad, T. K.; Lim, D.-W. Hydrogen Storage in Metal–Organic Frameworks. *Chem. Rev.* **2012**, *112*, 782–835.

- (5) Sumida, K.; Rogow, D. L.; Mason, J. A.; McDonald, T. M.; Bloch, E. D.; Herm, Z. R.; Bae, T.-H.; Long, J. R. Carbon Dioxide Capture in Metal–Organic Frameworks. *Chem. Rev.* **2012**, *112*, 724–781.
- (6) Makal, T. A.; Li, J.-R.; Lu, W.; Zhou, H.-C. Methane Storage in Advanced Porous Materials. *Chem. Soc. Rev.* **2012**, *41*, 7761–7779.
- (7) Eddaoudi, M.; Moler, D. B.; Li, H.; Chen, B.; Reineke, T. M.; O’Keeffe, M.; Yaghi, O. M. Modular Chemistry: Secondary Building Units as a Basis for the Design of Highly Porous and Robust Metal–Organic Carboxylate Frameworks. *Acc. Chem. Res.* **2001**, *34*, 319–330.
- (8) Eddaoudi, M.; Eubank, J. F. In *Metal–Organic Frameworks: Design and Application*; MacGillivray, L. R., Ed.; John Wiley & Sons, Inc.: Hoboken, NJ, 2010; pp 37–89.
- (9) Pham, T.; Forrest, K. A.; McLaughlin, K.; Tudor, B.; Nugent, P.; Hogan, A.; Mullen, A.; Cioce, C. R.; Zaworotko, M. J.; Space, B. Theoretical Investigations of CO₂ and H₂ Sorption in an Interpenetrated Square-Pillared Metal–Organic Material. *J. Phys. Chem. C* **2013**, *117*, 9970–9982.
- (10) Forrest, K. A.; Pham, T.; McLaughlin, K.; Belof, J. L.; Stern, A. C.; Zaworotko, M. J.; Space, B. Simulation of the Mechanism of Gas Sorption in a Metal–Organic Framework with Open Metal Sites: Molecular Hydrogen in PCN-61. *J. Phys. Chem. C* **2012**, *116*, 15538–15549.
- (11) Caskey, S. R.; Wong-Foy, A. G.; Matzger, A. J. Dramatic Tuning of Carbon Dioxide Uptake via Metal Substitution in a Coordination Polymer with Cylindrical Pores. *J. Am. Chem. Soc.* **2008**, *130*, 10870–10871, PMID: 18661979.
- (12) Burd, S. D.; Ma, S.; Perman, J. A.; Sikora, B. J.; Snurr, R. Q.; Thallapally, P. K.; Tian, J.; Wojtas, L.; Zaworotko, M. J. Highly Selective Carbon Dioxide Uptake by [Cu(bpy-n)₂(SiF₆)]ⁿ (bpy-1 = 4,4'-Bipyridine; bpy-2 = 1,2-Bis(4-pyridyl)ethene). *J. Am. Chem. Soc.* **2012**, *134*, 3663–3666.
- (13) Nugent, P.; Belmabkhout, Y.; Burd, S. D.; Cairns, A. J.; Luebke, R.; Forrest, K.; Pham, T.; Ma, S.; Space, B.; Wojtas, L.; Eddaoudi, M.; Zaworotko, M. J. Porous Materials with Optimal Adsorption Thermodynamics and Kinetics for CO₂ Separations. *Nature* **2013**, *495*, 80–84.
- (14) Mohamed, M. H.; Elsaidi, S. K.; Wojtas, L.; Pham, T.; Forrest, K. A.; Tudor, B.; Space, B.; Zaworotko, M. J. Highly Selective CO₂ Uptake in Uninodal 6-Connected “mmo” Nets Based upon MO₄²⁻ (M = Cr, Mo) Pillars. *J. Am. Chem. Soc.* **2012**, *134*, 19556–19559.
- (15) Ma, S.; Sun, D.; Simmons, J. M.; Collier, C. D.; Yuan, D.; Zhou, H.-C. Metal–Organic Framework from an Anthracene Derivative Containing Nanoscopic Cages Exhibiting High Methane Uptake. *J. Am. Chem. Soc.* **2008**, *130*, 1012–1016.
- (16) Wu, H.; Zhou, W.; Yildirim, T. High-Capacity Methane Storage in Metal–Organic Frameworks M₂(dhtp): The Important Role of Open Metal Sites. *J. Am. Chem. Soc.* **2009**, *131*, 4995–5000.
- (17) Guo, Z.; Wu, H.; Srinivas, G.; Zhou, Y.; Xiang, S.; Chen, Z.; Yang, Y.; Zhou, W.; O’Keeffe, M.; Chen, B. A Metal–Organic Framework with Optimized Open Metal Sites and Pore Spaces for High Methane Storage at Room Temperature. *Angew. Chem., Int. Ed.* **2011**, *50*, 3178–3181.
- (18) He, Y.; Zhou, W.; Krishna, R.; Chen, B. Microporous Metal–Organic Frameworks for Storage and Separation of Small Hydrocarbons. *Chem. Commun.* **2012**, *48*, 11813–11831.
- (19) Liu, D.; Wu, H.; Wang, S.; Xie, Z.; Li, J.; Lin, W. A high Connectivity Metal–Organic Framework with Exceptional Hydrogen and Methane Uptake Capacities. *Chem. Sci.* **2012**, *3*, 3032–3037.
- (20) Li, B.; et al. Enhanced Binding Affinity, Remarkable Selectivity, and High Capacity of CO₂ by Dual Functionalization of a rht-Type Metal–Organic Framework. *Angew. Chem., Int. Ed.* **2012**, *51*, 1412–1415.
- (21) Wang, X.-J.; Li, P.-Z.; Chen, Y.; Zhang, Q.; Zhang, H.; Chan, X. X.; Ganguly, R.; Li, Y.; Jiang, J.; Zhao, Y. A Rationally Designed Nitrogen-Rich Metal–Organic Framework and Its Exceptionally High CO₂ and H₂ Uptake Capability. *Sci. Rep.* **2013**, DOI: 10.1038/srep01149.
- (22) Burchell, T.; Rogers, M. Low Pressure Storage of Natural Gas for Vehicular Applications. *SAE Technol. Pap. Ser.* **2000**, *1*, 2000–2205.
- (23) ARPA-E: Funding Opportunity Exchange. 2013; <https://arpa-e-foa.energy.gov> (Accessed August 9, 2013).
- (24) Peng, Y.; Krungleviciute, V.; Eryazici, I.; Hupp, J. T.; Farha, O. K.; Yildirim, T. Methane Storage in Metal–Organic Frameworks: Current Records, Surprise Findings, and Challenges. *J. Am. Chem. Soc.* **2013**, *135*, 11887–11894.
- (25) Chen, B.; Ockwig, N. W.; Millward, A. R.; Contreras, D. S.; Yaghi, O. M. High H₂ Adsorption in a Microporous Metal–Organic Framework with Open Metal Sites. *Angew. Chem., Int. Ed.* **2005**, *117*, 4823–4827.
- (26) Lin, Q.; Wu, T.; Zheng, S.-T.; Bu, X.; Feng, P. Single-Walled Polytetrazolate Metal–Organic Channels with High Density of Open Nitrogen-Donor Sites and Gas Uptake. *J. Am. Chem. Soc.* **2012**, *134*, 784–787.
- (27) Xue, D.-X.; Cairns, A. J.; Belmabkhout, Y.; Wojtas, L.; Liu, Y.; Alkordi, M. H.; Eddaoudi, M. Tunable Rare-Earth fcu-MOFs: A Platform for Systematic Enhancement of CO₂ Adsorption Energetics and Uptake. *J. Am. Chem. Soc.* **2013**, *135*, 7660–7667.
- (28) Kizzie, A. C.; Wong-Foy, A. G.; Matzger, A. J. Effect of Humidity on the Performance of Microporous Coordination Polymers as Adsorbents for CO₂ Capture. *Langmuir* **2011**, *27*, 6368–6373.
- (29) Nugent, P.; Rhodus, V.; Pham, T.; Tudor, B.; Forrest, K.; Wojtas, L.; Space, B.; Zaworotko, M. Enhancement of CO₂ Selectivity in a Pillared pcu MOM Platform through Pillar Substitution. *Chem. Commun.* **2013**, *49*, 1606–1608.
- (30) Mohamed, M. H.; Elsaidi, S. K.; Pham, T.; Forrest, K. A.; Tudor, B.; Wojtas, L.; Space, B.; Zaworotko, M. J. Pillar Substitution Modulates CO₂ Affinity in “mmo” Topology Networks. *Chem. Commun.* **2013**, *49*, 9809–9811.
- (31) Zaworotko, M. J. Crystal Engineering of Diamondoid Networks. *Chem. Soc. Rev.* **1994**, *23*, 283–288.
- (32) Evans, O. R.; Xiong, R.-G.; Wang, Z.; Wong, G. K.; Lin, W. Crystal Engineering of Acentric Diamondoid Metal–Organic Coordination Networks. *Angew. Chem., Int. Ed.* **1999**, *38*, 536–538.
- (33) Hoskins, B. F.; Robson, R. Infinite Polymeric Frameworks Consisting of Three Dimensionally Linked Rod-Like Segments. *J. Am. Chem. Soc.* **1989**, *111*, 5962–5964.
- (34) Hoskins, B.; Robson, R. Design and Construction of a New Class of Scaffolding-Like Materials Comprising Infinite Polymeric Frameworks of 3D-Linked Molecular Rods. A Reappraisal of the Zinc Cyanide and Cadmium Cyanide Structures and the Synthesis and Structure of the Diamond-Related Frameworks [N(CH₃)₄]⁺[Cu^IZn^{II}(CN)₄]⁻ and Cu^I[4,4',4'',4''-Tetracyanotetraphenylmethane]⁻BF₄⁻_xC₆H₅NO₂. *J. Am. Chem. Soc.* **1990**, *112*, 1546–1554.
- (35) Evans, O. R.; Wang, Z.; Xiong, R.-G.; Foxman, B. M.; Lin, W. Nanoporous, Interpenetrated Metal–Organic Diamondoid Networks. *Inorg. Chem.* **1999**, *38*, 2969–2973.
- (36) Lin, W.; Ma, L.; Evans, O. R. NLO-active Zinc (II) and Cadmium (II) Coordination Networks with 8-Fold Diamondoid Structures. *Chem. Commun.* **2000**, 2263–2264.
- (37) Evans, O. R.; Lin, W. Crystal Engineering of Nonlinear Optical Materials Based on Interpenetrated Diamondoid Coordination Networks. *Chem. Mater.* **2001**, *13*, 2705–2712.
- (38) Evans, O. R.; Lin, W. Crystal Engineering of NLO Materials Based on Metal–Organic Coordination Networks. *Acc. Chem. Res.* **2002**, *35*, 511–522.
- (39) Elsaidi, S. K.; Mohamed, M. H.; Wojtas, L.; Chanthapally, A.; Pham, T.; Space, B.; Vittal, J. J.; Zaworotko, M. J. Putting the Squeeze on CH₄ and CO₂ through Control over Interpenetration in Diamondoid Nets. *J. Am. Chem. Soc.* **2014**, *136*, 5072–5077.
- (40) Farrusseng, D.; Daniel, C.; Gaudillere, C.; Ravon, U.; Schuurman, Y.; Mirodatos, C.; Dubbeldam, D.; Frost, H.; Snurr, R. Q. Heats of Adsorption for Seven Gases in Three Metal–Organic Frameworks: Systematic Comparison of Experiment and Simulation. *Langmuir* **2009**, *25*, 7383–7388.
- (41) Yuan, D.; Zhao, D.; Sun, D.; Zhou, H.-C. An Isoreticular Series of Metal–Organic Frameworks with Dendritic Hexacarboxylate Ligands and Exceptionally High Gas-Uptake Capacity. *Angew. Chem., Int. Ed.* **2010**, *122*, 5485–5489.

- (42) Dincă, M.; Dally, A.; Liu, Y.; Brown, C. M.; Neumann, D. A.; Long, J. R. Hydrogen Storage in a Microporous Metal-Organic Framework with Exposed Mn²⁺ Coordination Sites. *J. Am. Chem. Soc.* **2006**, *128*, 16876–16883.
- (43) Myers, A. L.; Prausnitz, J. M. Thermodynamics of Mixed-Gas Adsorption. *AIChE J.* **1965**, *11*, 121–127.
- (44) Metropolis, N.; Rosenbluth, A. W.; Rosenbluth, M. N.; Teller, A. H.; Teller, E. Equation of State Calculations by Fast Computing Machines. *Phys. Lett. B* **1953**, *21*, 1087–1092.
- (45) Frenkel, D.; Smit, B. *Understanding Molecular Simulation: From Algorithms to Applications*; Academic Press: New York, 2002.
- (46) Peng, D.-Y.; Robinson, D. B. A New Two-Constant Equation of State. *Ind. Eng. Chem. Fundam.* **1976**, *15*, 59–64.
- (47) Ewald, P. P. Die Berechnung optischer und elektrostatischer Gitterpotentiale. *Ann. Phys.* **1921**, *369*, 253–287.
- (48) Belof, J. L.; Stern, A. C.; Eddaoudi, M.; Space, B. On the Mechanism of Hydrogen Storage in a Metal-Organic Framework Material. *J. Am. Chem. Soc.* **2007**, *129*, 15202–15210.
- (49) Pham, T.; Forrest, K. A.; Nugent, P.; Belmabkhout, Y.; Luebke, R.; Eddaoudi, M.; Zaworotko, M. J.; Space, B. Understanding Hydrogen Sorption in a Metal-Organic Framework with Open-Metal Sites and Amide Functional Groups. *J. Phys. Chem. C* **2013**, *117*, 9340–9354.
- (50) Forrest, K. A.; Pham, T.; Hogan, A.; McLaughlin, K.; Tudor, B.; Nugent, P.; Burd, S. D.; Mullen, A.; Cioce, C. R.; Wojtas, L.; Zaworotko, M. J.; Space, B. Computational Studies of CO₂ Sorption and Separation in an Ultramicroporous Metal-Organic Material. *J. Phys. Chem. C* **2013**, *117*, 17687–17698.
- (51) Siperstein, F.; Myers, A.; Talu, O. Long Range Corrections for Computer Simulations of Adsorption. *Mol. Phys.* **2002**, *100*, 2025–2030.
- (52) Jorgensen, W. L.; Maxwell, D. S.; Tirado-Rives, J. Development and Testing of the OPLS All-Atom Force Field on Conformational Energetics and Properties of Organic Liquids. *J. Am. Chem. Soc.* **1996**, *118*, 11225–11236.
- (53) Rappé, A. K.; Casewit, C. J.; Colwell, K. S.; Goddard, W. A.; Skiff, W. M. UFF, a Full Periodic Table Force Field for Molecular Mechanics and Molecular Dynamics Simulations. *J. Am. Chem. Soc.* **1992**, *114*, 10024–10035.
- (54) Mullen, A. L.; Pham, T.; Forrest, K. A.; Cioce, C. R.; McLaughlin, K.; Space, B. A Polarizable and Transferable PHAST CO₂ Potential for Materials Simulation. *J. Chem. Theory Comput.* **2013**, *9*, 5421–5429.
- (55) Cioce, C. R.; Tudor, B.; McLaughlin, K.; Belof, J. L.; Space, B. A PHAST Potential for Heterogeneous Simulation of Methane with Many-Body Interactions. Manuscript in preparation, 2014.
- (56) Potoff, J. J.; Siepmann, J. I. Vapor-Liquid Equilibria of Mixtures Containing Alkanes, Carbon Dioxide, and Nitrogen. *AIChE J.* **2001**, *47*, 1676–1682.
- (57) Martin, M. G.; Siepmann, J. I. Transferable Potentials for Phase Equilibria. 1. United-Atom Description of n-Alkanes. *J. Phys. Chem. B* **1998**, *102*, 2569–2577.
- (58) Nicholson, D.; Parsonage, N. G. *Computer Simulation and the Statistical Mechanics of Adsorption*; Academic Press: London, 1982.
- (59) Pan, H.; Ritter, J. A.; Balbuena, P. B. Examination of the Approximations Used in Determining the Isosteric Heat of Adsorption from the Clausius–Clapeyron Equation. *Langmuir* **1998**, *14*, 6323–6327.
- (60) Belof, J. L.; Space, B. Massively Parallel Monte Carlo (MPMC). Available on Google Code, 2012.